Design of porous silica from hybrid organic–inorganic precursors

Pierre Chevalier,[a] Robert J. P. Corriu,*[,a] Pierre Delord,[b] Joël J. E. Moreau*[,c] and Michel Wong Chi Man[c]

[a] *Laboratoire de Chimie Moléculaire et Organisation du Solide (CNRS UMR 44), Université Montpellier II, Place E. Bataillon, 34095 Montpellier cédex 5, France*
[b] *Groupe de Dynamique des Phases Condensées (CNRS UMR 5581), Université Montpellier II, Place E. Bataillon, 34095 Montpellier cédex 5, France*
[c] *Laboratoire de Chimie Organométallique (CNRS ESA 5076), Ecole Nationale Supérieure de Chimie, 8, Rue de l'Ecole Normale, 34296 Montpellier cédex 5, France*

Hybrid organic-inorganic silica-based materials containing a labile bridging organic unit have been prepared. The elimination of the organic fragment is possible under very mild conditions at room temperature in the presence of a small amount (2%) of fluoride ion as catalyst. The silicas obtained after chemical treatment have been compared with those obtained by a sacrificial route (oxidation at 600 °C in air). The mild cleavage of Si—C bonds eliminates the organic units and generates mesoporous silicas with a very narrow pore size distribution (45 Å). In contrast, the high temperature air oxidation gave a microporous silica with a wide dispersion of pore diameters. There is a big difference between the sizes of the pores and the size of the organic molecule eliminated. A discrepancy between the sizes of the pores in silicas resulting from the chemical elimination and the sacrificial oxidation route is also observed. A rearrangement of the hybrid network to form a pure silica network takes place during the elimination of the organic moities.

Sol-gel-derived hybrid organic-inorganic materials are receiving much attention since they can exhibit the properties associated with both the organic moities and the inorganic framework.[1] The preparation of a molecularly defined hybrid network consisting of alternating organic and siloxane units was achieved by sol-gel hydrolysis of suitable precursors containing one non-hydrolyzable silicon—carbon bond.[1g,2,3] This approach is of particular interest since it might allow controlled formation of the three-dimensional network based on the structure of the molecular precursor.[4]

Recent work has also pointed out the potential of organic-inorganic hybrids for the controlled preparation of purely inorganic amorphous materials after elimination of the organic component. The use of organic molecules and self-assembled organic aggregates as structure-directing agents led to micro- and mesoporous alumino-silicate materials.[5] Whereas this strategy is well-suited to prepare crystalline zeolites, the design preparation of amorphous materials is more complex. Attempts have been made to control the pore size of silica *via* the temporary introduction of organic polymers in the silicate matrix. The removal of the template then led to porous oxide.[6] It is essential that the intermediate hybrid material be homogeneous and exhibit no phase separation. The pore size of porous silica was successfully controlled, by the size of the organic component used, upon pyrolysis of a hybrid containing a starburst dendrimer.[7] Related molecular imprinting also constitutes an attractive approach for the design of selective catalysts.[8,9]

The tailoring of the pore structure of a material would be best achieved from a homogeneous molecularly defined hybrid network. The use of silsesquioxane hybrids as the inorganic material precursor is therefore of particular interest.[10–12] The elimination of the organic fragment in a silsesquioxane network was achieved using an oxidation reaction.[11]

As shown in Scheme 1, the plasma oxidation of hydrocarbon templates led to silica showing a coarsening of the existing porosity. Compared to the hybrid precursor, the post-plasma material had a higher average pore diameter and a lower surface area. The plasma treatment opened up the walls of the existing pores to form mesoporous silicas.

We recently showed that hybrid silsesquioxane gels containing acetylenic bridging units[3a,12] led to silica upon treatment with MeOH–H_2O in the presence of ammonium fluoride as catalyst (Scheme 2). The fragile Si—C_{sp} bond allowed the

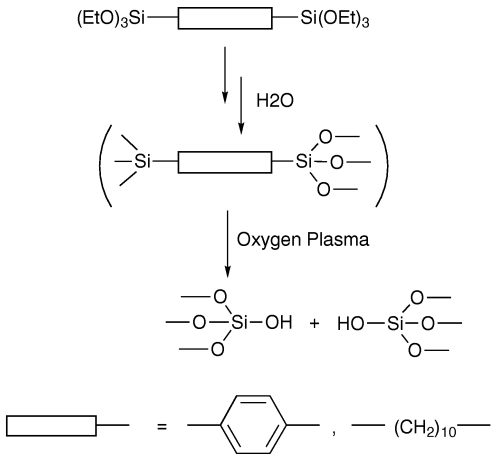

Scheme 1 Oxidation of hydrocarbon templates in poly (silsesquioxanes)[11]

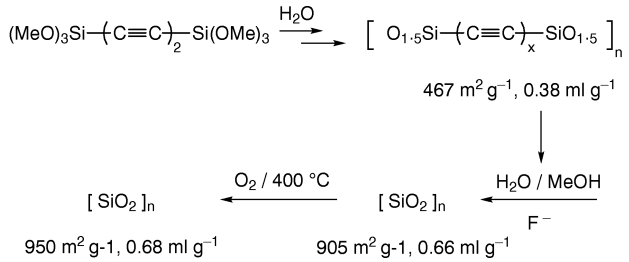

Scheme 2 Mild removal of the organic fragment in acetylenic bridged silsesquioxanes

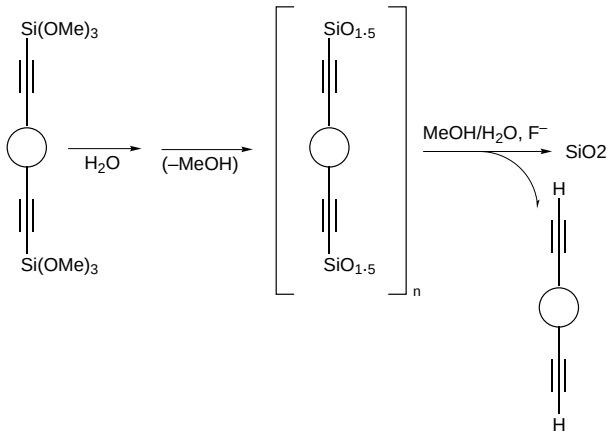

Scheme 3 Mild preparation of silicas from silsesquioxane gels containing template bridging fragments

removal of the acetylenic molecule under mild reaction conditions upon NH_4F catalysed hydrolysis. The resulting silica had a surface area and pore volume higher than those of the hybrid precursor. This led us to examine the possible design of the pore structure in inorganic materials by a non-sacrificial route in two steps (Scheme 3). First a silsesquioxane gel is prepared from an appropriate precursor in which the organic fragment is attached through a labile Si—C bond. Then mild recovery of the organic template gives the silica.

We wish to report here the use of a linear rigid spacer as the template molecule. We studied the pore structure of the post-cleavage silicas as a function of the structure of the hybrid network. We compared the elimination methods: chemical cleavage of the Si—C bond *vs.* air oxidation of the organic fragment. We wish to show that the use of a mild selective removal of the organic moiety allowed us to generate mesoporous materials with a narrow pore size distribution, which can be varied according to the amount of organic content in the hybrid gel precursor.

Results and Discussion

1 Preparation and characterisation of hybrid silsesquioxane materials

We first prepared a linear rigid spacer containing a para-phenylene unit:

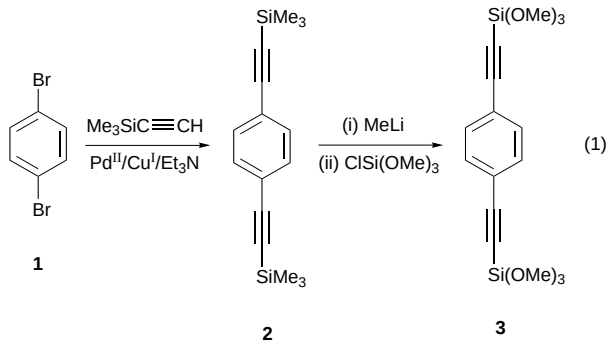

It was obtained in two steps from *p*-dibromobenzene **1**. The trimethylsilyl derivative **2** was first prepared by a Sonogashira coupling reaction using trimethylsilylacetylene in the presence of palladium catalyst.[13] Then the nucleophilic cleavage of the Si—C bond with MeLi generates a dilithium diacetylide, which upon condensation with $ClSi(OMe)_3$ led to the functionalized bis(trimethoxysilyl) precursor **3**. The latter was formed quantitatively from the easily purified intermediate **2**.

The hydrolysis and condensation of **3** was then performed under mild conditions in THF by adding a stoichiometric amount of water at room temperature. Gelation occurred within a few minutes and the resulting gel was allowed to

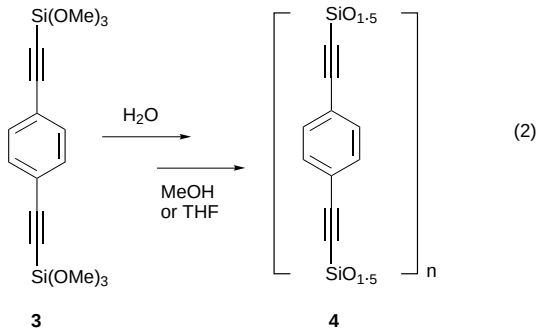

stand for 8 days to allow further condensation reaction. It was then powdered, washed with solvents and dried *in vacuo* at room temperature.

The collected hybrid material **4** was characterised by IR and NMR spectroscopy. As shown in Fig. 1 the ^{13}C MAS NMR spectra showed the resonances associated with the organic fragment: two lines at 123 and 132 ppm associated with the aromatic carbon atoms and two lines at 90 and 102 ppm, which can be assigned to the two acetylenic carbon atoms. Residual uncondensed methoxy groups in the solid material also showed a resonance at 51 ppm. The ^{29}Si MAS NMR spectrum also provides interesting information. The set of signals at −79, −87 and −95 ppm is characteristic of a silicon atom attached to three oxygen and one sp carbon atoms.[12,14] As observed in previous cases with related materials, a major T^2 [$CSi(OH))(OSi)_2$ or $CSi(OMe)(OSi)_2$] substructure is observed and minor resonances corresponding to T^1 [$CSi(OH)_2(OSi)$ or $CSi(OMe)_2(OSi)$] and T^3 [$CSi(OSi)_3$] appeared. From the NMR spectra the structure of the hybrid network can be described as siloxane chains with bridging phenylenediynylene units and with, on average, one uncondensed OH or OMe group per silicon.

We prepared also hybrid gels upon co-hydrolysis and condensation of the acetylenic bis(trimethoxysilyl) precursor **3** in the presence of variable amounts of $Si(OMe)_4$. This led to hybrid gels with increasing dispersion and dilution of the organic fragment into the silicate network. The hydrolysis of a mixture of **3** with 2–8 mol equivalent of $Si(OMe)_4$ was performed in THF as previously and led to the hybrid gels **5**–**8**.

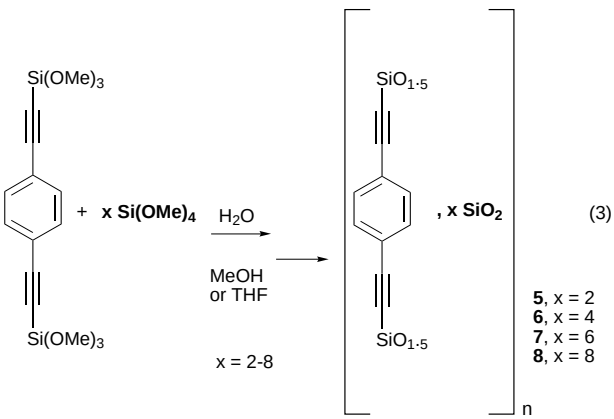

These were characterized by FTIR and MAS NMR spectroscopies. The ^{13}C solid state NMR spectra showed the expected ^{13}C resonance associated with the bridging organic fragment. The ^{29}Si MAS NMR spectra exhibited two sets of signals associated with T ($CSiO_3$) and Q (SiO_4) substructures arising from the hydrolysis-polycondensation of **3** and $Si(OMe)_4$. The major resonance corresponds to T^2 [$CSi(OH)(OSi)_2$ or $CSi(OMe)(OSi)_2$] and Q^3 [$Si(OH)(OSi)_3$ or $Si(OMe)(OSi)_3$] substructures. Fig. 1 shows the ^{13}C and ^{29}Si NMR spectra of the hybrid silica gel **6** obtained by using four moles of $Si(OMe)_4$ as an example.

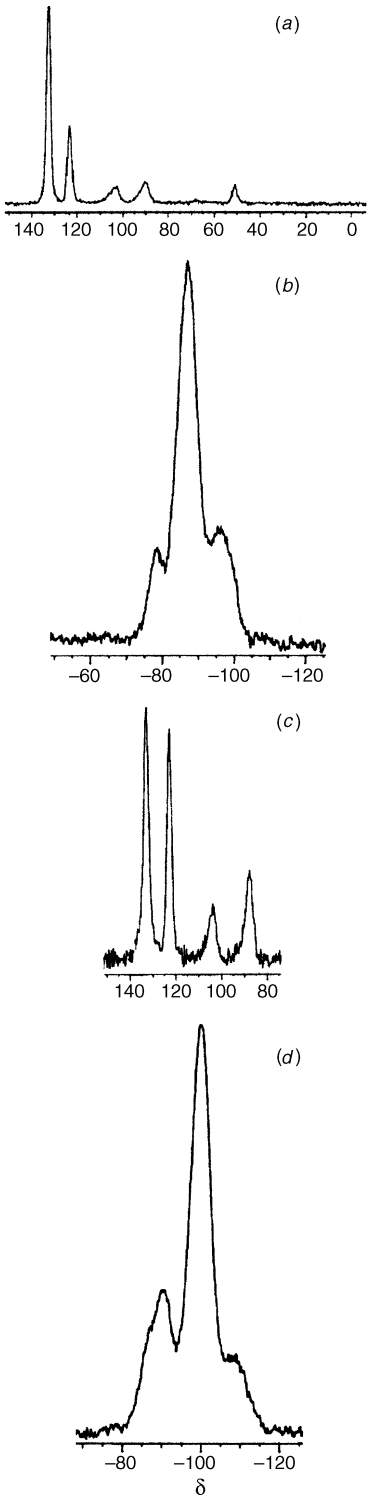

Fig. 1 (*a*) ^{13}C CP TOSS NMR and (*b*) ^{29}Si CP MAS NMR spectra of hybrid gel **4**. (*c*) ^{13}C CP TOSS NMR and (*d*) ^{29}Si CP MAS NMR spectra of hybrid gel **6** obtained by hydrolysis of a mixture of **3** with 4 moles of $Si(OMe)_4$

2 Elimination of the organic fragment in the hybrid gels

The hybrid materials were then treated by two different methods to eliminate the organic fragment: (*i*) mild hydrolytic cleavage of the Si—C bond or (*ii*) direct high temperature air oxidation of the hybrid material.

2.1 Mild cleavage of the Si—C bond. A suspension of the hybrid gel **4** in MeOH was treated with water in the presence of 2% ammonium fluoride as catalyst (Scheme 4). After heating gently, 1,4-diethynylbenzene was isolated from the methanol solution and the solid silica residue **9A** was collected by filtration, washed and dried. The ^{13}C NMR spectrum of the solid is consistent with a complete cleavage of the Si—C bonds in the material and elimination of the organic moities. The ^{29}Si NMR spectrum only showed resonances due to SiO_4 units, in agreement with complete Si—C bond cleavage. Major Q^3 [$Si(OH)(OSi)_3$ or $Si(OMe)(OSi)_3$] and Q^4 [$Si(OSi)_4$] substructures were formed during the reaction, which occurs in the solid state. This means that the Si—C bond cleavage is accompanied by further condensation in the material to form new Si—O—Si linkages.

The silica **9A** first produced (Scheme 4) upon mild cleavage contained some residual carbon corresponding to non-hydrolysed uncondensed methoxy groups. A carbon-free silica material **9B** could then be obtained upon heating **9A** in air at 600 °C for a few hours. Silicas **9A** and **9B** showed very similar ^{13}C and ^{29}Si solid state NMR spectra with major Q^3 and Q^4 substructures.

Comparison of the ^{29}Si NMR spectra of the hybrid gel **4** and post-cleavage silicas **9** shows that an important rearrangement occurred in the solid state during the elimination of the organic template molecule. As shown in Scheme 5, the organic bridging fragment is replaced by a siloxane bridge and additional condensation also occurs.

A similar mild treatment was carried out to eliminate the organic bridging unit in the hybrid gels **5**–**8** (Scheme 6). In all

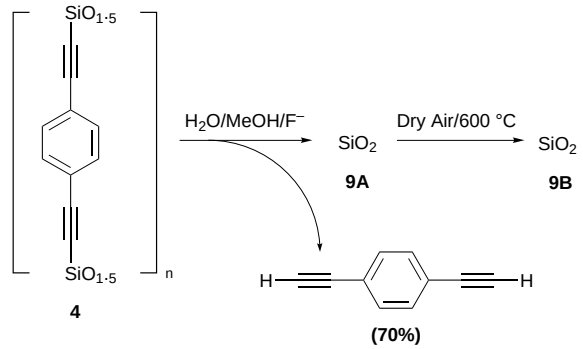

Scheme 4 Mild hydrolytic cleavage of Si—C bonds in hybrid gel **4**

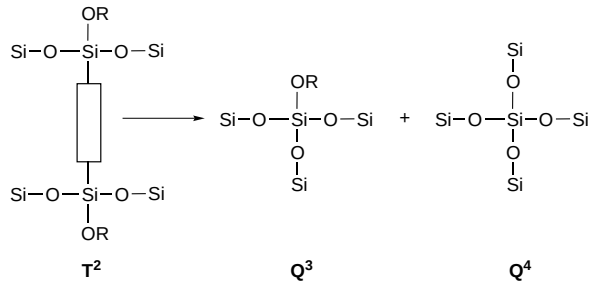

Scheme 5 Si—C Bond cleavage and rearrangement in the hybrid network

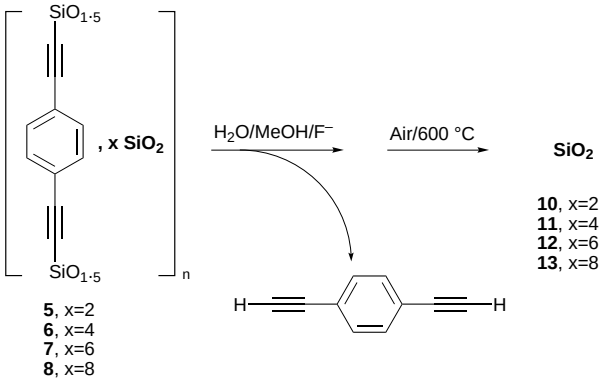

Scheme 6 Si—C Bond cleavage in hybrid co-gels **5**–**8**

cases complete cleavage and recovery of the organic moieties was obtained. The post-cleavage silicas arising from mild hydrolysis also contained some residual uncondensed methoxy groups and the carbon-free silicas **10**–**13** were then produced after heating the samples in air at 600 °C for 2–4 h. The various silicas obtained showed NMR spectra consistent with a complete cleavage of Si—C bond in the hybrid network and complete elimination of the organic diyne unit.

2.2 High temperature oxidation of the organic template. For comparison we also studied the high temperature sacrificial removal of the organic component. It was achieved upon heating the hybrid material up to 600 °C in air for 3–4 h (Scheme 7). Pure carbon free silicas were produced upon direct calcination of the hybrid. The solid state NMR spectra were similar to those recorded with the samples arising from mild cleavage and subsequent heating at 600 °C. The ^{29}Si MAS NMR spectrum is in agreement with complete removal of the organic moieties and formation of SiO_4 substructures. The Q^3 and Q^4 resonances are, however, broader than in the case of the silicas **9**, indicating a presumably more cross-linked silica network.

3 Pore structure of post-cleavage silicas

3.1 Mild Si—C bond cleavage. The porosity and surface properties were determined using nitrogen adsorption according to the BET method.[15] The hybrid material has a low porosity and a surface area of 20 $m^2\ g^{-1}$ was measured in the case of gel **4**. The surface area, pore volume and average pore diameter of the silicas resulting from the cleavage of the various hybrid gels were also measured and the results are given in Table 1. The silicas produced have a high surface area, 640–750 $m^2\ g^{-1}$, and large pore volume (up to 0.8 $cm^3\ g^{-1}$). The values vary according to the nature of the hybrid solid.

It is first interesting to compare the observed values and the isotherms and t-plots recorded for silicas **9A** and **9B** arising from cleavage of hybrid gel **4** prepared by sol-gel hydrolysis condensation of pure **3**. The N_2 adsorption–desorption measurements are consistent with a mesoporous material with a narrow pore-size distribution. As shown in Fig. 2, the data recorded for silica **9A** arising from the low temperature cleavage of the organic fragment are quite similar with those recorded for silica **9B** produced upon further heating **9A** at 600 °C. This shows that the pore structure of the material generated at low temperature is stable and is not further modified upon heating at high temperature. In particular, the desorption pore volume plots revealed a similar narrow pore-size distribution with average pore diameters of 50 and 46 Å. Similar observations have been made with silicas **10**–**13** arising from the cleavage of hybrid gels **5**–**8** prepared by co-hydrolysis of **3** and variable amounts of $Si(OMe)_4$.

It is also interesting to compare the pore structure of the silicas that result from the mild cleavage of hybrid gels **5**–**8** as a function of the amount of $Si(OMe)_4$ used in the co-hydrolysis condensation of **3**. Fig. 3 shows only the desorption pore volume plots of the various silica materials. Mesoporous materials with a narrow pore size distribution are obtained in all cases. The average pore diameter varies from 46 to 24 Å and decreases with increasing amount of $Si(OMe)_4$ used in the preparation of the hybrid solid precursor. At the same time, some porosity appeared in the micropore domain. According to the composition of the hybrid gel, the pore structure of the post-cleavage silicas can be varied between two limits: 46 Å corresponding to the gel made using the pure organic precursor **3** and 23 Å corresponding to silica made by hydrolysis of pure $Si(OMe)_4$ under similar reaction conditions (Table 1).

It is noteworthy that the pore size is much larger than the size of the organic molecule that is eliminated. Nevertheless,

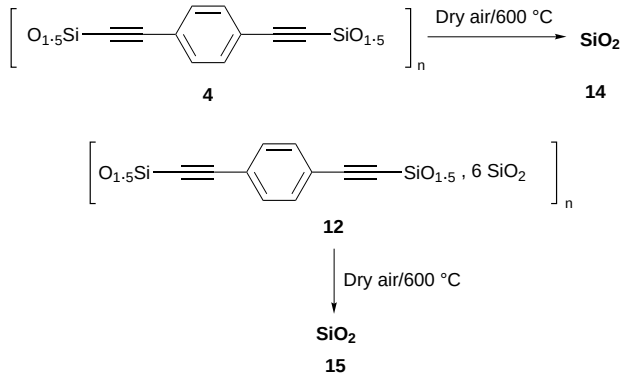

Scheme 7 Direct calcination of the hybrid material

the pores that are generated are very homogeneous in size. It seems that the rearrangement of the network taking place during the elimination of the organic molecule and the formation of the pores occurs in a controlled way to give a solid with a very homogeneous pore structure. The homogeneous pore size distribution is confirmed by transmission electron micrographs of the silica materials. Comparison of the photographs of the hybrid material and that of the post-cleavage silicas showed a homogeneously distributed porosity. Fig. 4 shows the TEM micrographs of hybrid gels **4** and **7**, of post-cleavage silicas **9** and **12** and of post-calcination silicas **14** and **15** as examples.

3.2 Sacrificial oxidation of the organic template. It is of interest to compare the pore structure of the above material with that of a similar material formed using a high temperature sacrificial route. That is to say, a silica produced by direct heating of the hybrid material in air at 600 °C. We therefore studied the thermal oxidation of hybrid gel **4** and **7** arising, respectively, from the hydrolysis condensation of the organic precursor **3** alone and in the presence of 6 mol equivalents of $Si(OMe)_4$. The carbon-free silicas obtained in this case were microporous materials. The isotherm, t-plots and desorption pore volume plots are shown in Fig. 5. They are characteristic of a microporous material in which the main pore volume is less than 20 Å. It is noteworthy that quite similar microporous solids are formed upon thermal treatment of both hybrid gels **4** and **7** to give silicas **14** and **15** (*cf.* Fig. 5, Table 1). The composition of the hybrid precursor does not seem to influence the pore structure of the post-oxidation

† The SAXS technique is sensitive to the fluctuations of electronic density in the medium more precisely, it is the Fourier transform of the self-correlation of these fluctuations. In the case of a porous medium, it may be supposed that such a medium consists of two phases, of constant electronic density, respectively the solid silica skeleton and the pores. The scattered intensity I is then proportional to the square of the so-called contrast term which is the difference between the two densities.[16] The contrast between the solid and the air in the pores is high and therefore the scattered intensity is strong enough. A plot of the Neperian logarithm of the scattered intensity ln (I) *vs.* ln (q) where q is the scattering vector defined by $q = 4\pi\sin\theta/\lambda$ (λ is the wavelength of the X-rays and 2θ the scattering angle) is often used for presentation of the results. Generally speaking, mainly three domains are to be considered. At low values of q, an overall size of the scattering object may be achieved by the co-called Guinier law, which gives a gyration radius of the scattering object, mainly in the case of dilute media. For concentrated media, and for powder samples at very low q, the meaning of such a radius is very doubtful.[16,17]

At intermediate q values, the rate of decay is determined by the dimensionality of the structure: for example, rodlike objects give a q^{-1} slope. If it is supposed that the rod is long enough with respect to its section, a plot of $\ln[qI(q)]$ *vs.* q^2 allows us to determine a radius of gyration of the cylindrical section supposed constant and circular.[16,17]

At high values of q, the intensity follows Porod's law with a slope of q^{-4} for smooth particles or interfaces.

materials. One can imagine that the thermal treatment at high temperature caused a drastic rearrangement to form the silica network and that control of the pore structure can only result from a mild and selective cleavage of the hybrid network.

3.3 Small angle X-ray scattering studies. In order to confirm the results we have studied the porosities of porous silicas using small angle X-ray scattering (SAXS)†.

The spectra of silicas **9A** and **9B** are very similar (Fig. 6): they are quite superimposable over the whole scanned domain. This is a good indication that pyrolysis at 600 °C of the material after mild removal of the organic fragment does not affect significantly the structure of the porous medium.

A plot $\ln(q \times I)$ *vs.* q^2 shows a bimodal behavior that allows us to determine two diameters (Fig. 7) from the slope. The largest diameters, 42 Å for **9A** and 41 Å for **9B** [Fig. 7 (top)], agree with the pore diameters issued from the BET experiments (see Table 1). The smallest diameters 32 and 34 Å, respectively, for silicas **9A** and **9B** [Fig. 7 (bottom)] might be assigned to the solid phase surrounded by pores; further experiments are necessary to support this explanation.

Table 1 Surface and porosity properties of post-cleavage silicas **9–13** and post-calcination silicas **14** and **15**[a]

Silicas	Surface area /$m^2\ g^{-1}$	Pore volume /$cm^3\ g^{-1}$	Pore diameter /Å
(**9A**)	656	0.83	50.5
(**9B**)	657	0.76	46.4
(**10**)	713	0.68	38.0
(**11**)	710	0.53	30.0
(**12**)	639	0.41	25.6
(**13**)	639	0.38	23.5
$(SiO_2)^b$	516	0.30	23.0
14	430	0.21	14.6
15	271	0.14	15.2

[a] BET surface area from multipoint analysis of the N_2 adsorption isotherm. [b] Silica prepared under similar reaction conditions by hydrolysis polycondensation of $Si(OMe)_4$.

A q^{-4} slope of the spectrum at high q values is observed and indicates a clear cut change in density between the solid silica phase and the void following Porod's law. The silica obtained after direct high temperature treatment (600 °C)

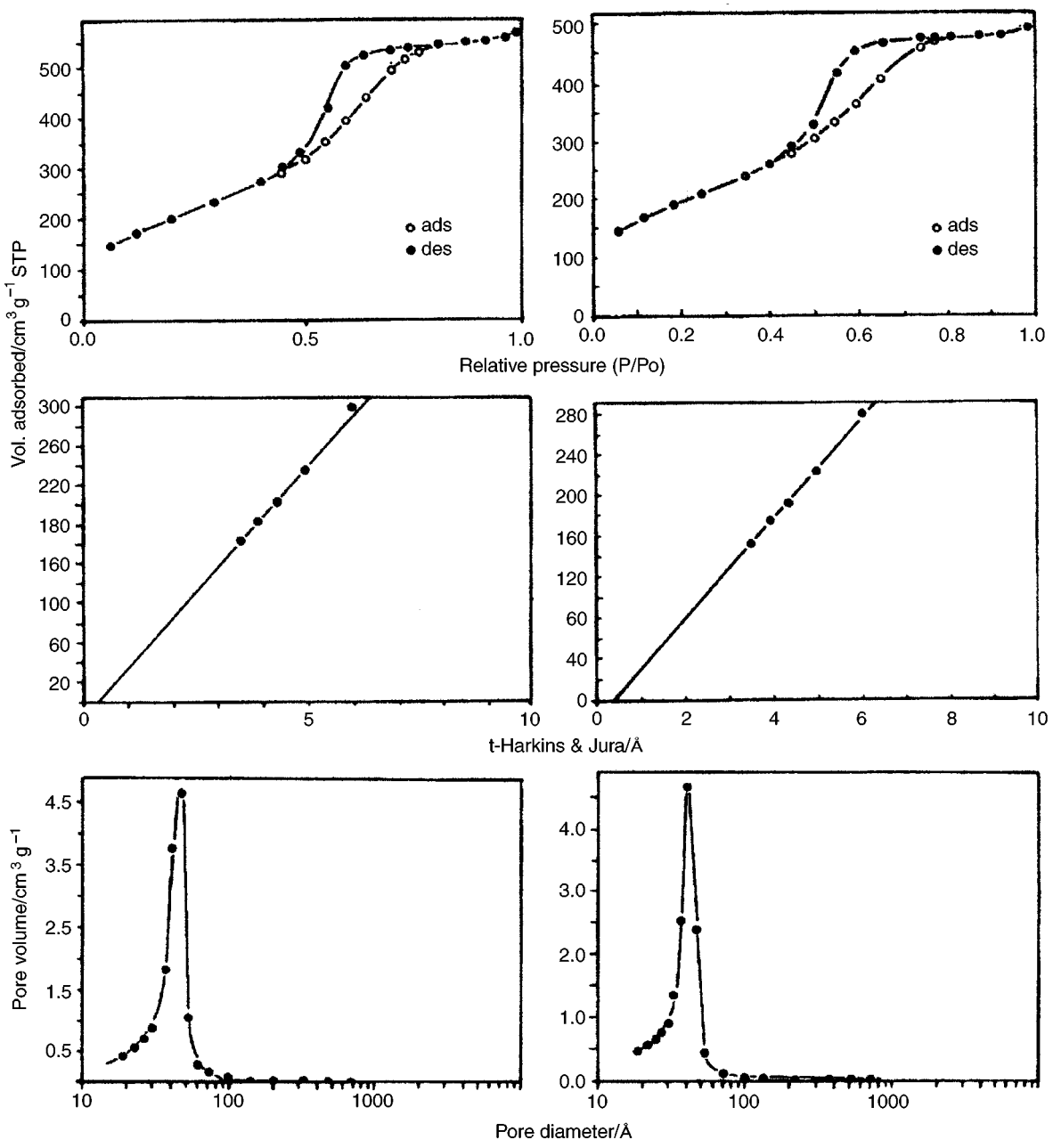

Fig. 2 Isotherm plots (top), t-plots (middle) and desorption pore volume plots (bottom) of silicas **9A** (left) and **9B** (right)

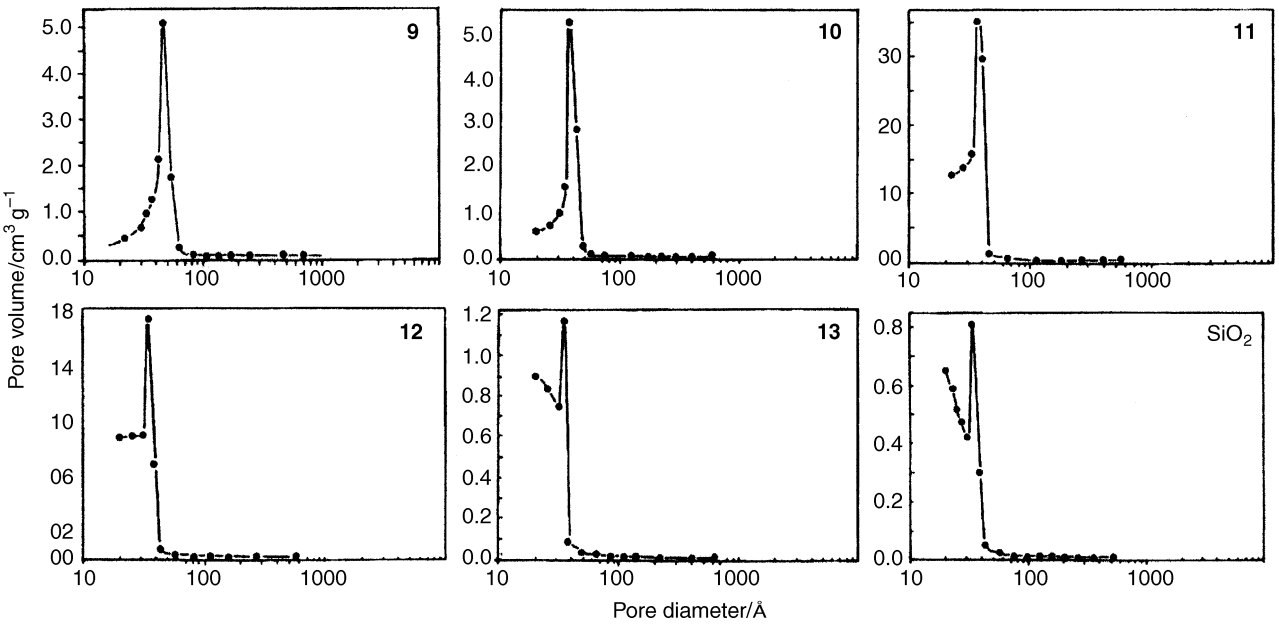

Fig. 3 Desorption pore volume plots of gels **9**–**13** and SiO_2

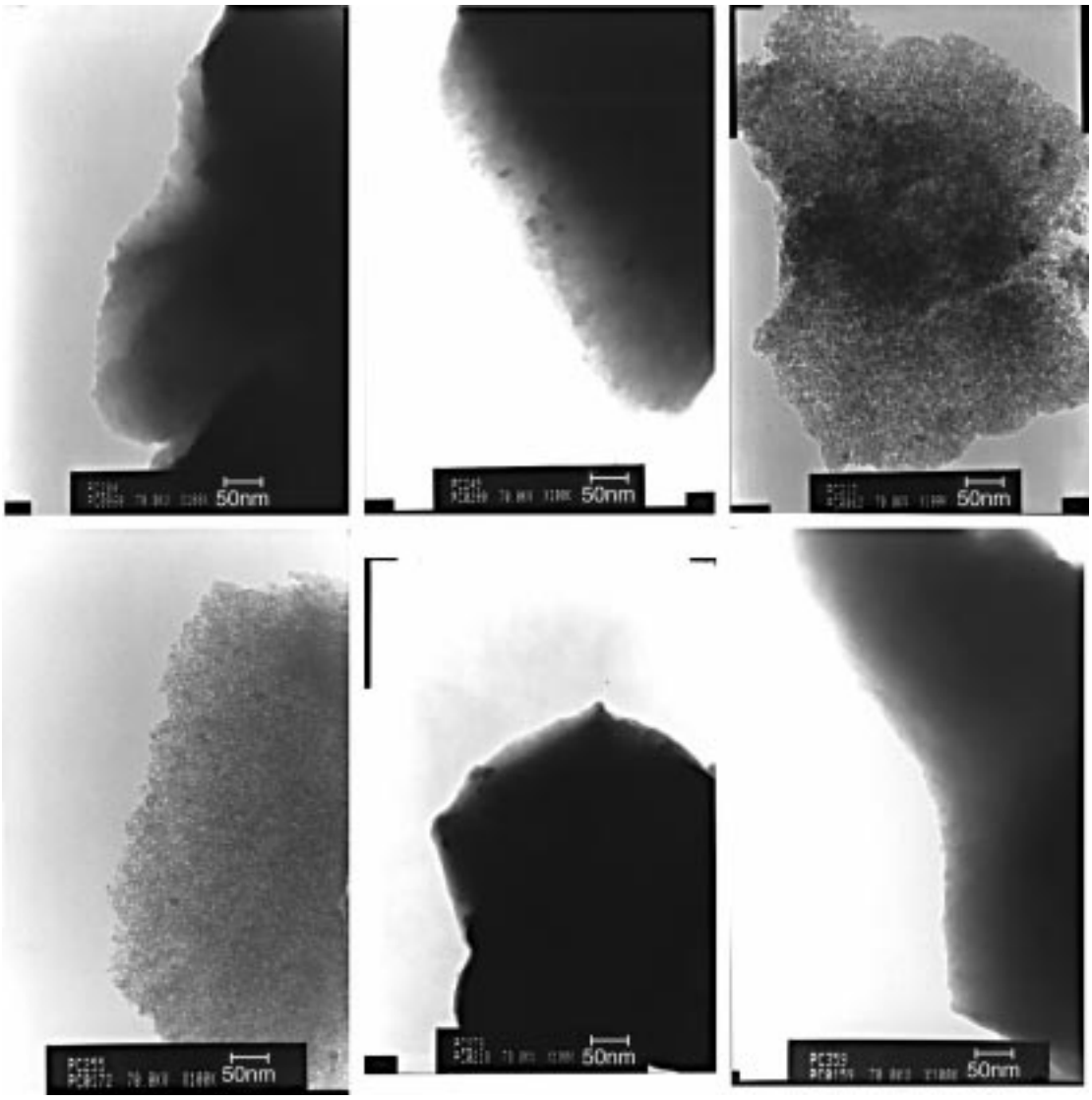

Fig. 4 TEM micrographs of materials **4**, **7**, **9** (top; left, centre, right), **12**, **14** and **15** (bottom; left, centre, right)

exhibits a completely different feature. The spectrum (Fig. 8) does not show classical behaviour: a power law in $q^{-3.2}$ is observed, suggesting the possibility of a surface fractal behaviour. Comparison with silica **9A** shows that the structure of the porous medium is very different when obtained by mild hydrolytic cleavage of the Si—C bond or by direct high tem-

perature oxidation.

Thus, the porosities obtained with the BET method are confirmed by SAXS: (1) a narrow dispersion with similar values of the pore size obtained by chemical treatment; (2) similarity of the solid obtained after chemical treatment followed or not by thermal treatment (600 °C in air) and (3) a very different solid obtained by direct thermal treatment of the hybrid material.

4 Discussion

From the above results, it appears possible to vary the pore structure of the post-cleavage material by varying the composition of the hybrid network precursor. The pore structure is quite homogeneous in size in all cases and the average pore diameter decreases as the dispersion of the organic fragment in the hybrid network increase. The pore structure is the result of the cleavage and rearrangement of the hybrid network to form a purely inorganic network. The rearrangement that takes place at low temperature occurs step-by-step in the solid state. As shown from solid state NMR studies, the hybrid network containing a major T^2 structure is rearranged to a silica network containing more condensed units corresponding to Q^3 and Q^4 structures. As illustrated in Scheme 8, the reaction takes place first by nucleophilic coordination at the central silicon atom followed by cleavage of the Si—C bond during the nucleophilic attack of H_2O. This reaction involving nucleophilic catalysis by fluoride ion is a well-documented process in organosilicon chemistry.[18,19] Upon Si—C bond cleavage Q^2 [$Si(OH)_2(OSi)_2$] substructures are generated; these condense with another silicon atom in the vicinity, leading to Q^3 [$Si(OH)(OSi)_3$] substructures and inducing a second Si—C bond cleavage. Therefore, such a step-by-step cleavage condensation reaction leads to the elimination of the organic acetylenic molecule and generates a purely inorganic silicate network.

The pore size observed is larger than the size of the organic moieties. This discrepancy can be explained by two factors.

The first one is the reorganisation of the silica network catalysed by F^- occurring during the cleavage and after the cleavage. It is possible that the presence of F^- could induce a reorganisation of the SiO_2. This reorganisation is evidenced by the presence of Q^3 and Q^4 units in the final SiO_2 network. The rearrangement occurs in the solid state with a restricted mobility of the cross-linked siloxane chains. The pore structure will therefore be influenced by the structural properties of the three-dimensional network and particularly by the degree of cross-linking and condensation of the hybrid network. The rearrangement is probably controlled by the rigid properties of the network, which vary depending on the composition of the hybrid material, produced by hydrolysis of either pure organometallic precursors or those containing increasing amounts of $Si(OMe)_4$.

The second one is the possible auto-organisation occurring between the organic units during the polycondensation reaction. The affinity between the organic moieties could promote a short-range organisation to give aggregates that might be, at least partly, responsible for the bigger size of the pores compared to the size of one molecule. The pore structure is very homogeneous because the hybrid is very homogeneous and well-defined at the molecular level and because the mild reactions involved take place in a similar way in the whole solid material.

The high temperature oxidation generates a silica material with completely different morphological properties, which do not seem to be dependent on the nature or composition of the hybrid network. The drastic reaction conditions in this case will lead to a similar material upon rearrangement of the network.

Experimental

All reactions were carried out under nitrogen by use of a vacuum line and Schlenk tube techniques or three-neck flasks. Solvents were dried and distilled before use. The reported yields refer to pure isolated materials. Melting points were determined with a Gallenkamp apparatus and are uncorrected. IR spectra were recorded by using a Perkin Elmer 1600 FTIR spectrometer. ^1H NMR spectra were recorded on Bruker AW 80 and Bruker AC 250 spectrometers; ^{13}C and ^{29}Si NMR spectra both in solution and in the solid state were recorded on a Bruker WP 250 FT AM 300 apparatus. Solvents and chemical shifts (δ relative to Me_4Si) are indicated. Mass spectra were measured on a Jeol JMS-DX 300 mass spectrometer (ionization energy of 70 eV).

Thermogravimetric and differential analysis (TGA-TDA) were performed under flowing air (50 mL min^{-1}) with a Netzsch STA 409 thermobalance; the typical heating rate was 10 °C min^{-1}. The pyrolysis experiments were performed under dry air in a tubular Carbolite furnace with internal Eurotherm

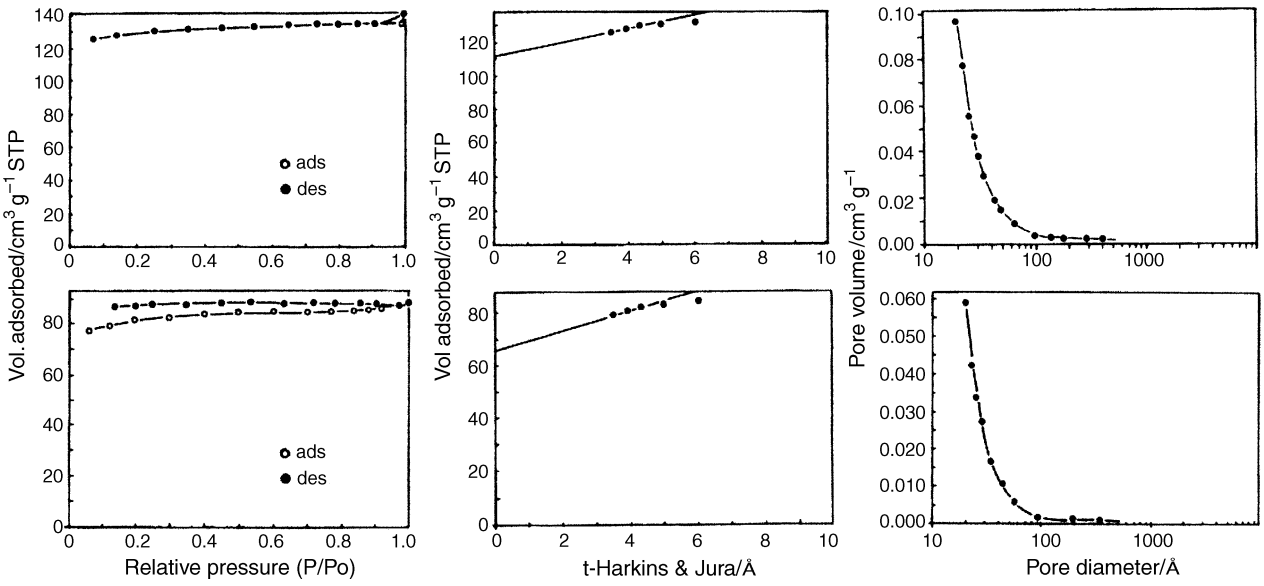

Fig. 5 Isotherm plots (left), t-plots (middle) and desorption pore volume plots (right) of post-calcination silicas **14** (top) and **15** (bottom)

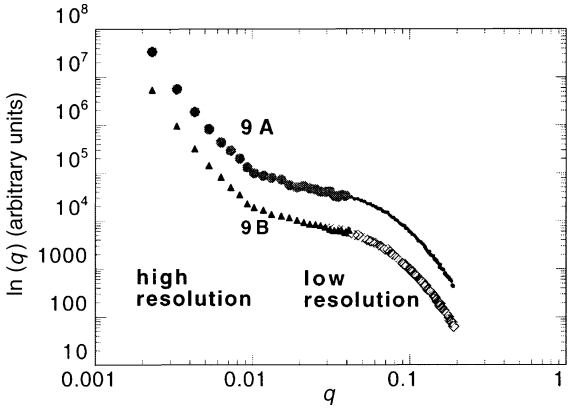

Fig. 6 Silicas **9A** and **9B**. Intensity in arbitrary units *vs.* the scattering vector q (log scale)

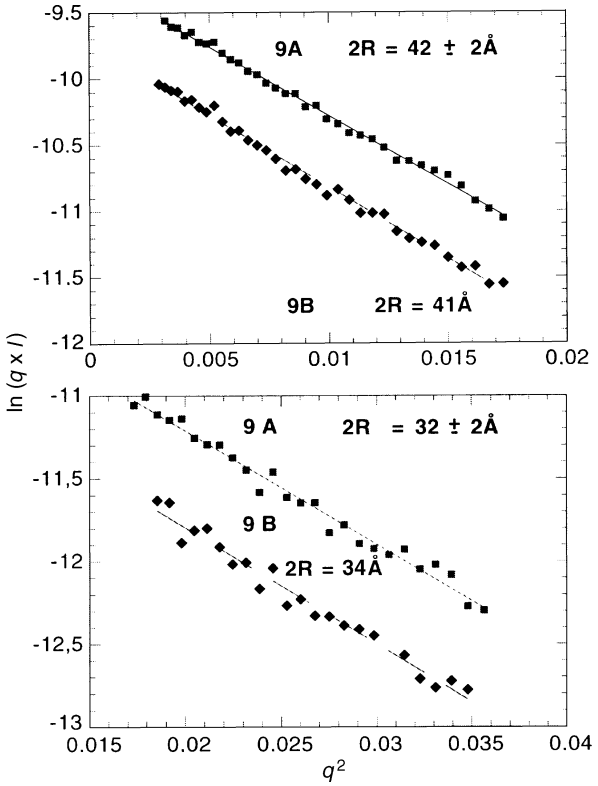

Fig. 7 Silicas **9A** and **9B**. Radius of an elongated cylinder: $\ln(q \times I)$ *vs.* q^2

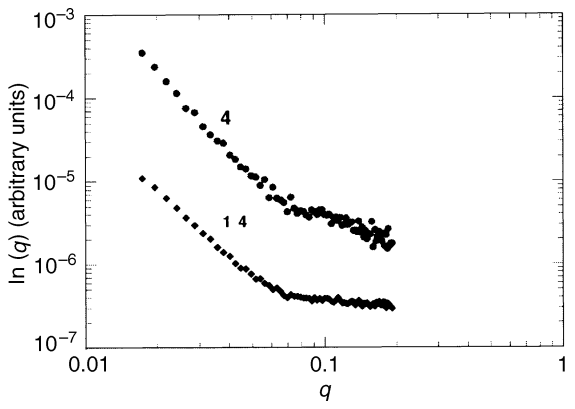

Fig. 8 Hybrid gel **4** and post-calcination silica **14**: intensity *vs.* scattering vector q (log scale)

programming and were carried out by pouring weighed samples of solids into an aluminum oxide boar place in an aluminum oxide tube connected to a vacuum line. Gas flow was maintained at around 50 mL min^{-1} during pyrolysis. The surface areas, porous volume and the pore size distribution were determined by analyzing the N_2 adsorption–desorption isotherms according to the BET method using a Micromeritic ASAP 2400 apparatus. X-Ray powder diffraction measurements were performed using a Seifert M24 apparatus. Elemental analysis (%) were carried out by the 'Service Central de Micro-analyse du CNRS'. The photographs of solids were obtained by transmission electron micrography (TEM) using a JEM 1200 EX2 apparatus. SAXS experiments were carried out on a high resolution Bonse–Hart camera with two germanium channel cuts[20] for very small q values [three reflections on (111) planes for each crystal] and on a low resolution classical apparatus with a Ge (111) monochromator and a linear detector for q values above 0.03 $Å^{-1}$. The wavelength was 1.542 Å (Cu Kα radiation) and the specimens were powdered and dried samples. The spectra were deconvoluted with adapted procedures.

Preparations

1,4-Bis(trimethysilylethynyl)benzene 2. To a solution of 43.6 g (184.8×10^{-3} mol) of 1,4-dibromobenzene, 5.18 g (7.4×10^{-3} mol) of $(Ph_3P)_2PdCl_2$ and 0.97 g (5.1×10^{-3} mol) of CuI in 700 mL of NEt_3 were added dropwise *via* a syringe 47.2 g (481.2×10^{-3} mol) of commercial trimethylsilylacetylene. A precipitate formed at room temperature. The yellow-brown reaction mixture became greenish and then brown-red by heating 12 h at 40 °C under vigorous stirring. The resulting mixture was filtered and the salts extracted with hexane–CCl_4. The solvent was removed under reduced pressure, the viscous liquid residue was purified on a chromatographic column (support: 500 g of 70–230 mesh silica; eluant: toluene–CCl_4 5 : 3). After evaporation of the solvents, the solid was recrystallized in hexane to give 46.90 g (94% yield) of compound **2**. Bright colourless plaques: mp 122.9–123.3 °C; IR (CCl_4, ν cm^{-1}): 1251, 1496, 2159, 2900, 2962; ^1H NMR (CCl_4, δ): 0.05 (18H, s), 7.17 (4H, s); MS (EI) *m/z* 270 (45%, M^+), 255 (100, $M^+ - Me$), 225 (6, $M^+ - 3Me$), 210 (2, $M^+ - 4Me$), 73 (13, Me_3Si^+); Anal. calcd for $C_{16}H_{22}Si_2$: C, 71.04; H, 8.20; found: C, 71.00; H, 8,21.

1,4-Bis(trimethoxysilylethynyl)benzene 3. To a solution of 3.0 g (11.1×10^{-3} mol) of **2** in 20 mL of THF cooled at −40 °C is added dropwise, *via* an addition funnel, 16.3 mL of MeLi · Br in excess dissolved in ether ([MeLi] = 1.5 M) under stirring. The reaction mixture was then heated 30 min at 40 °C until an insoluble light grey dianion formed. This suspension in THF was then cooled at −50 °C and poured dropwise *via* a metallic pipe into a solution of 3.8 g (24.3×10^{-3} mol, in excess) of $ClSi(OMe)_3$ prepared as previously described[21] in 20 mL of THF kept at −70 °C. After this addition the reaction mixture was heated at room temperature. Solvents and TMS were pumped off and extraction with pentane of the residue, filtration and evaporation of the solvent led to a viscous yellow liquid. Distillation of the new residue (160 °C, 2×10^{-2} mbar) afforded 2.55 g (63% yield) of compound **3**. Pale yellow liquid: IR (CCl_4, ν cm^{-1}): 1108, 1498, 2170, 2844, 2944; ^1H NMR (CCl_4, δ): 3.41 (18H, s), 7.29 (4H, s); ^{13}C NMR ($CDCl_3$, δ): 51.29 (q), 86.42 (s), 104.07, 122.99 (s), 132.66 (d); ^{29}Si NMR ($CDCl_3$, δ): 69.52; MS (EI): *m/z* 366 (100%, M^+), 335 (28, $M^+ - OMe$), 305 (6, $M^+ - 2OMe$), 90 [10, $Si(OMe)_2^+$]; Anal. calcd for $C_{16}H_{22}O_6Si_2$: C, 52.43; H, 6.05; found: C, 52.59; H, 5.95.

Hydrolysis and polycondensation of 1,4-bis(trimethoxysilylethynyl)benzene: hybrid gel 4. To 20.80 g (56.7×10^{-3} mol) of **3** in 18.9 mL of THF was added 3.06 mL

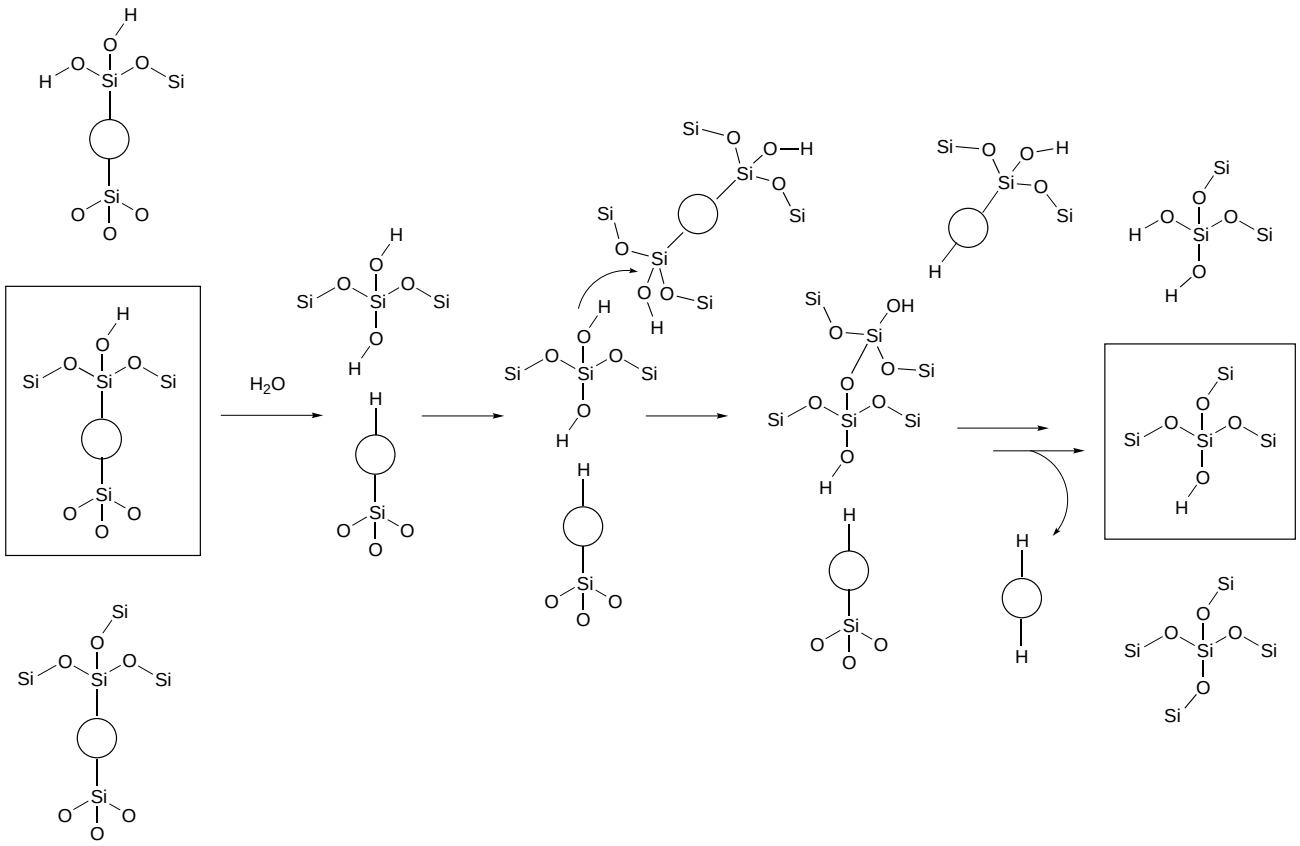

Scheme 8 Si—C Cleavage and rearrangement of the hybrid network

(170.1×10^{-3} mol, 3 mole equiv.) of distilled water. The homogeneous solution was allowed to stand at 20 °C until gelation. A monolithic, transparent pale-yellow gel formed within 60 s. After curing at 20 °C for one week in a closed vessel, the gel was powdered. The solid collected was washed with ether, filtered and dried *in vacuo* at room temperature over 24 h, yielding 15.74 g of a pale yellow powder corresponding to the xerogel **4**. IR (KBr, ν cm^{-1}): 1066, 1499, 2172, 2878, 2977, 3425; ^{13}C CP TOSS NMR (1300 scans, δ): 50.6, 89.9, 102.5, 123.1, 132.3; ^{29}Si CP MAS NMR (δ): −78.8, −87.2, −96.6; Anal. calcd for $C_{10}H_4O_3Si_2$: C, 52.61; H, 1.77; O, 21.02; Si, 24.60; found: C, 49.96; H, 4.04; O, 23.70; Si, 21.70 corresponding to $C_{10.77}H_{10.38}O_{3.83}Si_2$. BET surface area: 19 m^2 g^{-1}.

Hydrolysis and polycondensation of 1,4-bis(trimethoxysilylethynyl)benzene 3 and tetramethoxysilane. Hybrid cogel 5. To 8.47 g (23.1×10^{-3} mol) of **3** and 6.88 mL (46.2×10^{-3} mol, 2 mole equiv.) of tetramethoxysilane in 13.31 mL of THF was added 2.91 mL (161.7×10^{-3} mol, 7 mole equiv.) of distilled water. The homogeneous solution was allowed to stand at 20 °C until gelation. A monolithic transparent gel formed within 2.5 min. After curing at 20 °C for a week in a closed vessel, the gel was powdered. The solid was washed with ether, filtered and dried *in vacuo* at room temperature over 24 h, yielding 10.21 g of xerogel **5**. IR (KBr, ν cm^{-1}): 1069, 1500, 2174, 2856, 2987, 3448; ^{13}C CP TOSS NMR (δ): 51.3, 89.5, 103.5, 123.0, 132.4; ^{29}Si CP MAS NMR (δ): −79.4, −88.0, −99.2, −106.3; Anal. calcd for $C_{10}H_4O_7Si_4$: C, 34.47; H, 1.16; O, 32.14; Si, 32.23; found: C, 35.68; H, 3.83; O, 37.41; Si, 27.30 corresponding to $C_{12.22}H_{15.64}O_{9.62}Si_2$. BET surface area: 36 m^2 g^{-1}.

Hybrid cogel 6. Prepared as above using 5.88 g (16.0×10^{-3} mol) of **2**, 9.51 mL (64.0×10^{-3} mol) of tetramethoxysilane and 3×10^{-1} mol H_2O, the sol-gel hydrolysis yielded 9.45 g of xerogel **6**. IR (KBr, ν cm^{-1}): 1069, 1502, 2177, 2985, 2987, 3450; ^{13}C CP TOSS NMR (δ): 51.4, 88.8, 104.2, 122.7, 132.6; ^{29}Si CP MAS NMR (δ): −79.4, −89.7, −99.6, −106.3; Anal. calcd for $C_{10}H_4O_{11}Si_6$: C, 25.63; H, 0.86; O, 37.55; Si, 35.96; found: C, 26.02; H, 3.14; O, 37.81; Si, 30.10 corresponding to $C_{12.13}H_{17.44}O_{13.23}Si_6$. BET surface area: 16 m^2 g^{-1}.

Hybrid cogel 7. Prepared as above using 4.28 g (11.7×10^{-3} mol) of **2**, 10.43 mL (70.2×10^{-3} mol) of tetramethoxysilane and 3.2×10^{-1} mol H_2O, the sol-gel hydrolysis yielded 8.18 g of xerogel **7**. IR (KBr, ν cm^{-1}): 1066, 1502, 2179, 2986, 2987, 3455; ^{13}C CP TOSS NMR (δ): 50.5, 87.6, 103.7, 122.5, 132.7; ^{29}Si CP MAS NMR (δ): −90.4, −99.8, −108.5; Anal. calcd for $C_{10}H_4O_{15}Si_8$: C, 20.40; H, 0.68; O, 40.76; Si, 38.16; found: C, 22.51; H, 3.05; O, 40.01; Si, 30.70 corresponding to $C_{13.72}H_{22.15}O_{18.30}Si_8$. BET surface area: 9 m^2 g^{-1}.

Hybrid cogel 8. Prepared as above using 3.63 g (9.9×10^{-3} mol) of **2**, 11.77 mL (79.2×10^{-3} mol) of tetramethoxysilane and 3.5×10^{-1} mol H_2O, the sol-gel hydrolysis yielded 7.90 g of xerogel **8**. IR (KBr, ν cm^{-1}): 1074, 1502, 2178, 3448; ^{13}C CP TOSS NMR (δ): 50.6, 87.7, 103.9, 122.6, 132.8; ^{29}Si CP MAS NMR (δ); −9.10, −99.9, −108.8; Anal. calcd for $C_{10}H_4O_{19}Si_{10}$: C, 16.94; H, 0.57; O, 42.88; Si, 39.61; found: C, 19.39; H, 2.83; O, 46.50; Si, 32.65 corresponding to $C_{13.89}H_{24.15}O_{25.00}Si_{10}$. BET surface area: 6 m^2 g^{-1}.

Silica 9A (chemical treatment of 4). To 9.54 g (41.8×10^{-3} mol) of hybrid gel **4** was added 100 mL of distilled water, 40 mL of methanol and 0.84 mL (0.84×10^{-3} mol) of a 1 M solution of NH_4F. The reactive medium was refluxed at 75–80 °C under stirring for 4 days. The resulting solid was washed with THF and ether, filtered and dried *in vacuo* at room temperature over 24 h, yielding 4.85 g of ivory solid **9A**. The fil-

trate was purified by crystallization giving 2.81 g (65% yield) of *p*-diethnylbenzene. **9A**: IR (KBr, ν cm^{-1}): 1080, 2889, 3436; ^{13}C CP TOSS NMR (11 000 scans, δ): 50.8, ^{29}Si HPDEC NMR (δ): −90.7, −100.4, −110.8; Anal. calcd for SiO_2 : O, 53.26; Si 46.74; found: C, 7.47; H, 1.62; O, 45.92; Si, 39.50 corresponding to $C_{0.44}H_{1.14}O_{2.04}Si$. *p*-Diethynylbenzene: Bright colourless plates: mp: 95.8–96.4 °C; IR (CCl_4, ν cm^{-1}): 1494, 1506, 2113, 3306; ^1H NMR (CCl_4, δ): 2.89 (2H, s); 7.21 (4H, s); ^{13}C NMR ($CDCl_3$, δ): 79.51 (d); 83.41 (s); 122.93 (s); 132.41 (d); MS (EI): *m/z* 126 (100, M^+), 100 (30, $M^+ - C{\equiv}CH$), 76 (70, $M^+ - 2C{\equiv}CH$); Anal. calcd for $C_{10}H_6$: C, 95.21, H, 4.79; found: C, 94.29; H, 4.65.

Silica 9B (pyrolysis of solid 9A in air). Calcination under a dried air flow at 600 °C for 4 h of solid **9A** (3.03 g) led to 2.59 g of the white powder **9B**. IR (KBr, ν cm^{-1}): 1090, 3449; ^{29}Si HPDEC NMR (δ): −90.7, −101.3, −109.8; Anal. calcd for SiO_2 : O, 53.26; Si, 46.74; found: C, 0.16; H, 0.37; O, 54.92; Si, 46.20 corresponding to $C_{0.01}H_{0.22}O_{2.09}Si$. X-Ray analysis revealed an amorphous halo.

Pyrolysis of solid 4. Calcination under a dried air flow at 600 °C for 4 h of hybrid gel **4** (3.58 g) led to 1.59 g of the white powder **14**. IR (KBr, ν cm^{-1}); 1086, 3455; ^{29}Si HPDEC NMR (δ): −90.9, −101.7, −109.3; Anal. calcd for SiO_2 : O, 53.26; Si, 46.74; found: C, 1.41; H, 1.38; O, 53.96; Si 43.25 corresponding to $C_{0.08}H_{0.89}O_{2.19}$ Si; BET surface area: 433 m^2 g^{-1}; pore volume: 0.21 cm^3 g^{-1}; average pore diameter: 14.6 Å.

Silicas 10–13. These were obtained as described above in the case of silicas **9A** and **9B**. The characterisation data area as follows:

Silica 10. The treatment of gel **5** with MeOH in the presence of NH_4F gives after washing and drying a white solid: IR (KBr, ν cm^{-1}): 1090, 3452; ^{29}Si CP MAS NMR (δ): −90.5, −100.5, −110.1; Anal. calcd for SiO_2 : O, 53.26; Si, 46.74; found: C, 6.08; H, 2.02; O, 56.40 Si, 36.15 corresponding to $C_{0.39}H_{1.56}O_{2.74}Si$; BET surface area: 710 m^2 g^{-1}; pore volume: 0.71 cm^3 g^{-1}; average pore diameter: 40.0 Å. Heating in air at 600 °C for 4 h leads to silica **10**: IR (KBr, ν cm^{-1}): 1086, 3456; ^{29}Si CP MAS NMR (δ); −90.9, −100.1, −109.6; Anal. calcd for SiO_2 : O, 53.26; Si, 46.74; found: C, 0.69; H, 0.48; O, 52.413; Si 39.30 corresponding to $C_{0.04}H_{0.34}O_{2.33}$ Si.

Silica 11. The treatment of gel **6** with MeOH in the presence of NH_4F gives after washing and drying a white solid: IR (KBr, ν cm^{-1}): 1082, 3452; ^{29}Si NMR (δ): −91.1, −100.9, −110.1; Anal. calcd for SiO_2 : O, 53.26; Si, 46.74; found: C, 6.89; H, 2.18; O, 57.92; Si, 36.10 corresponding to $C_{0.45}H_{1.68}O_{2.82}Si$. BET surface area: 752 m^2 g^{-1}; pore volume: 0.58 cm^3 g^{-1}; average pore diameter: 30.09 Å. Heating in air at 600 °C for 4 h leads to silica **11**: IR (KBr, ν cm^{-1}): 1086, 3451; ^{29}Si CP MAS NMR (δ): −91.1, −99.3, −109.3; Anal. calcd for SiO_2 : O, 53.26; Si, 46.74; found: C, <0.10; H, 0.45; O, 51.94; Si 41.70 corresponding to $C_{<0.006}H_{0.30}O_{2.19}$ Si.

Silica 12. The treatment of gel **7** with MeOH in the presence of NH_4F gives after washing and drying a white solid: IR (KBr, ν cm^{-1}): 1089, 3464; ^{29}Si CP MAS NMR (δ): −90.8, −100.7, −110.1; Anal. calcd for SiO_2 : O, 53.26; Si, 46.74; found: C, 7.03; H, 2.10; O, 53.26; Si 34.35 corresponding to $C_{0.48}H_{1.70}O_{2.72}Si$. BET surface area: 699 m^2 g^{-1}; pore volume: 0.46 cm^3 g^{-1}; average pore diameter: 26.4 Å. Heating in air at 600 °C for 4 h leads to silica **12**: IR (KBr, ν cm^{-1}): 1082, 3456; ^{29}Si CP MAS NMR (δ): −91.2, −100.7, −109.6; Anal. calcd for SiO_2 : O, 53.26; Si, 46.74; found: C, 0.38; H, 1.18; O, 53.60; Si, 42.70 corresponding to $C_{0.02}H_{0.77}O_{2.20}$ Si.

Silica 13. The treatment of gel **8** with MeOH in the presence of NH_4F gives after washing and drying a white solid: IR (KBr, ν cm^{-1}): 1086, 3476; ^{29}Si CP MAS NMR (δ); −9.11, −100.9, −110.7; Anal. calcd for SiO_2 : O, 53.26; Si, 46.74; found: C, 7.29; H, 2.32; O, 51.20; Si, 39.10 corresponding to $C_{0.44}H_{1.65}O_{2.30}Si$. BET surface area: 906 m^2 g^{-1}; pore volume: 0.55 cm^3 g^{-1}; average pore diameter: 24.1 Å. Heating in air at 600 °C for 4 h leads to silica **13**: IR (KBr, ν cm^{-1}): 1086, 3475; ^{29}Si CP MAS NMR (δ): −91.5, −100.1, −109.4; Anal. calcd for SiO_2 : O, 53.26; Si, 46.74; found: C, 0.30; H, 0.35; O, 55.36; Si 43.99 corresponding to $C_{0.02}H_{0.22}O_{2.21}$ Si.

Pyrolysis of solid 8. Calcination under a dried air flow at 600 °C for 4 h of the hybrid cogel **8** (1.09 g) led to 0.73 g of the white powder **15**. IR (KBr, ν cm^{-1}): 1097, 3442; ^{29}Si HPDEC NMR (δ): −108.6; Anal. calcd for SiO_2 : O, 53.26; Si, 46.74; found: C, 0.34; H, 0.45; O, 53.71; Si, 45.50 corresponding to $C_{0.02}H_{0.28}O_{2.07}Si$. BET surface area: 271 m^2 g^{-1}; pore volume: 0.14 cm^3 g^{-1}; average pore diameter: 15.1 Å.

References

1 (*a*) H. K. Schmidt, *Mater. Res. Soc. Symp. Proc.*, 1984, **32**, 327; (*b*) H. K. Schmidt, *Inorganic and Organometallic Polymers*, ACS Symposium Series 360, American Chemical Society, Washington, DC, 1988, p. 333; (*c*) H. K. Schmidt, *Mater. Res. Soc. Symp. Proc.*, 1990, **180**, 961 and references therein; (*d*) J. D. MacKenzie, *J. Sol-Gel Sci. Tech.*, 1994, **2**, 81; (*e*) C. Sanchez and F. Ribot, *New J. Chem.*, 1994, **18**, 989; (*f*) U. Schubert, N. Hüsing and A. Lorenz, *Chem. Mater.*, 1995, **7**, 2010; (*g*) D. A. Loy and K. J. Shea, *Chem. Rev.*, 1995, **95**, 1431; (*h*) R. J. P. Corriu and D. Leclercq, *Angew. Chem., Int. Ed. Engl.*, 1996, **35**, 4001.

2 (*a*) K. J. Shea, D. A. Loy and O. W. Webster, *Chem. Mater.*, 1989, **1**, 574; (*b*) K. J. Shea, D. A. Loy and O. W. Webster, *J. Am. Chem. Soc.*, 1992, **114**, 6700 and references therein.

3 (*a*) R. J. P. Corriu, J. J. E. Moreau, P. Thépot and M. Wong Chi Man, *Chem. Mater.*, 1992, **4**, 1217; (*b*) R. J. P. Corriu, J. J. E. Moreau, P. Thépot and M. Wong Chi Man, *J. Sol-Gel Sci. Tech.*, 1994, **2**, 87.

4 G. Cerveau, C. Chorro, R. J. P. Corriu, C. Lepeytre, J. Lère-Porte, J. J. E. Moreau, P. Thépot and M. Wong Chi Man, *Hybrid Organic-Inorganic Composites*, ed. J. E. Mark, C. Y. C. Lee and P. A. Bianconi, ACS Symposium Series 585, American Chemical Society, Washington, DC, 1995, p. 210.

5 M. E. Davis, C. Y. Chen, S. L. Burkett and R. L. Lobo, *Mater. Res. Soc. Symp. Proc.*, 1994, **346**, 831 and references therein.

6 (*a*) T. Saegusa, *J. Macromol. Sect. Chem.*, 1991, **A28**, 817; (*b*) T. Saegusa and Y. Chujo, *Makromol. Chem. Symp.*, 1992, **64**, 1; (*c*) C. Roger, M. J. Hampden-Smith, D. W. Schaeffer and G. B. Beaucage, *J. Sol-Gel Sci. Tech.*, 1994, **2**, 67 and references therein; (*d*) N. K. Raman, M. T. Anderson and C. J. Brinker, *Chem. Mater.*, 1996, **8**, 1682 and references therein.

7 Y. Chujo, M. Matsuki, S. Kure, T. Saegusu and T. Yazawa, *J. Chem. Soc., Chem. Commun.*, 1994, 635.

8 (*a*) K. Morihara, S. Kurihar and J. Suzuki, *Bull. Chem. Soc. Jpn.*, 1988, **61**, 3991; (*b*) K. Morihara, M. Kurokawa, Y. Yamata and T. Shimada, *J. Chem. Soc., Chem. Commun.*, 1992, 356.

9 J. Heilmann and W. F. Maier, *Angew Chem., Int. Ed. Engl.*, 1994, **33**, 471.

10 (*a*) C. Roger, M. J. Hampden-Smith and C. Brinker, *J. Mater. Res. Symp. Proc.*, 1992, **271**, 51; (*b*) Y. Lu, G. Z. Cao, R. P. Kale, L. L. Delattre, C. J. Brinker and G. P. Lopez, *J. Mater. Res. Symp. Proc.*, 1996, **435**, 271.

11 D. A. Loy, R. J. Buss, R. A. Assink, K. J. Shea and H. Oiviatt, *Polym. Prepar. Am. Chem. Soc. Div. Polym. Chem.*, 1993, **34**, 244.

12 R. J. P. Corriu, J. J. E. Moreau, P. Thépot and M. Wong Chi Man, *Chem. Mater*, 1996, **100**, 8.

13 K. Sonogashira, *Comprehensive Organic Synthesis*, eds. D. Barton and W. D. Ollis, Oxford, UK, 1990, vol. 3, p. 521.

14 E. A. Williams, in *Chemistry of Organic Silicon Compounds*, eds. S. Patai and Z. Rappoport, Wiley, New York, 1989, p. 511.
15 (*a*) S. Brunauer, P. H. Emmett and E. J. Teller, *J. Am. Chem. Soc.*, 1938, **60**, 309; (*b*) E. P. Barrett, L. G. Joyner and P. P. Hallenda, *J. Am. Chem. Soc.*, 1951, **73**, 309.
16 A. Guinier, *Théorie et Techniques de la Radiocristallographie*, Dunod, Paris, 1956.
17 O. Glatter and O. Kratky, *Small Angle X-ray Scattering*, Academic Press, London, 1982.
18 R. J. P. Corriu, C. Guerin and J. J. E. Moreau, *Top. Curr. Chem.*, 1984, **15**, 43.
19 T. Kuwajima, E. Nakumura and K. Hashimoto, *Tetrahedron*, 1983, **39**, 975.
20 O. Bonse and M. Hart, in *Small Angle X-ray Scattering*, ed. H. Brumberger, Gordon and Breach Science Publishers, New York, 1967.
21 D. F. Peppard, W. G. Brown and W. C. Johnson, *J. Am. Chem. Soc.*, 1947, **68**, 70.

Received in Montpellier, France, 6th February 1998;
Paper 8/01407H